The Astrophysical Journal, 631:L105–L108, 2005 October 1

CONSTRAINING THE PHOTOMETRIC PROPERTIES OF Mg II–ABSORBING GALAXIES WITH THE SLOAN DIGITAL SKY SURVEY

Stefano Zibetti,[1] Brice Ménard,[2] Daniel Nestor,[3] and David Turnshek[4]

Received 2005 June 20; accepted 2005 August 25; published 2005 September 20

ABSTRACT

Using a sample of nearly 700 quasars with strong [$W_0(2796) > 0.8$ Å] Mg II absorption lines detected in the Early Data Release of the SDSS, we demonstrate the feasibility of measuring the photometric properties of the absorber systems by stacking SDSS imaging data. As Mg II lines can be observed in the range $0.37 < z_{\rm abs} < 2.2$, the absorbing galaxies are in general not identified in SDSS images, but they produce systematic light excesses around QSOs that can be detected with a statistical analysis. Here we present a 6 σ detection of this effect over the whole sample in the *i* band, rising to 9.4 σ for a low-redshift subsample with $0.37 < z_{\rm abs} \leq 0.82$. We use a control sample of QSOs without strong Mg II absorption lines to quantify and remove systematics with typical 10%–20% accuracy. The signal varies as expected as a function of absorber redshift. For the low-$z_{\rm abs}$ subsample, we can reliably estimate the average luminosities per Mg II absorber system in the *g*, *r*, and *i* bands, and we find them to be compatible with a stellar population a few hundred million years old at $M_r \sim -21$ in the rest frame. The colors are also consistent with typical absorbing galaxies resembling local Sb–c spirals. Our technique does not require any spectroscopic follow-up and does not suffer from confusion with other galaxies along the line of sight. It will be applied to larger samples and other line species in upcoming studies.

Subject headings: galaxies: photometry — galaxies: statistics — quasars: absorption lines — techniques: photometric

1. INTRODUCTION

A number of studies have inferred and then shown that strong metal absorption lines in a quasar spectrum are due to gaseous clouds associated with galaxies close to the line of sight (e.g., Bahcall & Spitzer 1969; Bergeron & Boissé 1991; Steidel et al. 1994). However, the systematic characterization of the emission properties of these absorber systems is still limited, especially at high redshifts (see, e.g., Churchill et al. 2005). In order to use absorption-line measurements to investigate galaxy formation and evolution, characterizing the underlying population of galaxies seen in absorption is an important task to achieve.

Among metal absorption lines, the Mg II doublet λλ2796, 2803, detectable from the ground at $0.2 < z < 2.2$, has been widely used. It arises in gas spanning more than 5 decades of neutral hydrogen column density (e.g., Churchill et al. 2000), and the strong systems, defined by $W_0(2796) \gtrsim 0.3$ Å, are found in the vicinity of galaxies spanning a large range of morphologies. Previous attempts to constrain the properties of Mg II absorbers have relied on deep imaging and spectroscopic follow-up of (arbitrarily faint) galaxies in the quasar field in order to identify a potential galaxy responsible for the absorption seen in the quasar spectrum. Such expensive studies have been limited to samples of a few tens of quasars.

Here we propose a new approach to measure the systematic photometric properties of large samples ($N \gg 100$) of absorbing systems, which combines statistical analysis of both spectroscopic and imaging data sets from the Sloan Digital Survey (SDSS; York et al. 2000). As Mg II lines can only be detected in SDSS spectra in the range $0.37 \lesssim z \lesssim 2.2$, the absorbing galaxies are not identified and, in general, are only marginally detected in individual SDSS images. However, they do produce systematic light excesses around the background QSOs that can be detected with a statistical analysis consisting of stacking a large number of absorbed QSO images. Such a statistical approach has already proved to be very powerful in detecting and characterizing the very low surface brightness *diffuse* light in galaxy halos (Zibetti et al. 2004) and the intracluster light (Zibetti et al. 2005). In this Letter, we demonstrate that significant detections can also be obtained with this technique for localized sources (the absorbing galaxies) in the presence of strong background contamination. Preliminary results on the photometric properties of the low-*z* (<0.82) absorbers are also analyzed. More detailed results and analysis for a larger sample will be presented in a forthcoming paper.

The paper is organized as follows: In § 1, we present the samples of QSOs used in our analysis. The image processing and stacking are described in § 2. The results are presented and analyzed in § 3, and concluding remarks and forthcoming developments are outlined in § 4. Standard ΛCDM cosmology ($\Omega_m = 0.3$, $\Omega_\Lambda = 0.7$) and $H_0 = 70$ km s^{-1} Mpc^{-1} are adopted throughout.

2. THE DATA

2.1. *The* Mg II *Absorber Sample*

We use the sample of Mg II absorption-line systems compiled by Nestor et al. (2005) and based on the SDSS Early Data Release (EDR; Stoughton et al. 2002). We focus our analysis only on strong systems, with a rest equivalent width $W_0(2796) > 0.8$ Å. In this range the detection completeness is above 95%. In this section, we briefly summarize the main steps involved in the absorption-line detection procedure. For details on the quasar and absorber catalogs, we refer the reader to Schneider et al. (2002) and Nestor et al. (2005). The SDSS EDR provides approximately 3700 QSO spectra of sufficiently high redshift

[1] Max-Planck-Institut für Extraterrestrische Physik, Postfach 1312, D-85741 Garching, Germany; szibetti@mpe.mpg.de

[2] Institute for Advanced Study, Einstein Drive, Princeton, NJ 08540; menard@ias.edu.

[3] Department of Astronomy, University of Florida, P.O. Box 112055, Gainesville, FL 32611; dbn@astro.ufl.edu.

[4] Department of Physics and Astronomy, University of Pittsburgh, 3941 O'Hara Street, Pittsburgh, PA 15260; turnshek@pitt.edu.

to allow the detection of intervening Mg II absorption lines. The continuum-normalized spectra were searched for Mg II λλ2796, 2803 doublets using automated routines and interactive confirmation or rejection of candidate systems. The rest equivalent widths W_0 of confirmed systems were measured using an optimal extraction method employing Gaussian line profiles (or more complex ones where appropriate). All systems were checked for blends and other special cases. A 5 σ significance level was required for all 2796 Å lines, as well as a 3 σ significance level for the corresponding 2803 Å lines. Only systems 0.1*c* blueward of the quasar redshift and redward of Lyα emission (so as to avoid the Lyα forest) were accepted. Systems with separations of less than 500 km s^{-1} were considered as a single system. In order to avoid confusion originating from the superposition of multiple absorbers along the same line of sight, we exclude from our sample all QSOs where distinct $W_0(2796) > 0.8$ Å absorber systems are detected; they represent 16.3% of the QSOs with $W_0(2796) > 0.8$ Å absorptions. The final sample comprises 683 QSOs, out of which two are excluded because they lie too close to bright stars. The absorber and QSO redshift distributions are shown in Figure 1.

2.2. *The Reference Quasar Sample*

In order to measure possible systematic light excess around QSOs that could contaminate the signal originating from absorbing galaxies, we use a control sample made of QSOs without strong absorbers. For each QSO with an absorber system, we randomly look for another QSO without any detected absorber down to $W_0(2796) = 0.8$ Å, such that their redshifts are matched within 0.1[5] and *i*-band brightnesses differ by less than 0.5 mag. In addition, we require that their spectra have similar signal-to-noise ratio (S/N) at the wavelengths corresponding to the Mg II absorption features. The last two conditions also imply that the average overall S/N per pixel in the spectra of the two samples differs by less than 0.1. Thus, our procedure ensures that (1) the probability of contamination by undetected Mg II systems along the line of sight is the same for both QSO sets and (2) photometric systematics that may possibly arise from residuals of the PSF subtraction (see §§ 2.1 and 3) affect both samples in the same way. Point 1 has also been verified by means of Monte Carlo simulations. The QSOs selected in this way are called *reference* QSOs in what follows. Their redshift distribution is also shown in Figure 1 (*dotted histogram*).

3. IMAGE STACKING

The image-stacking technique aims at producing a high-S/N *average* image of the QSOs, possibly surrounded by absorbing galaxies. It consists of four basic steps: (1) shifting to make images superposible, (2) intensity-rescaling to a uniform photometric calibration, (3) masking of all unwanted sources, and (4) average-combining of images, after rejecting masked regions. All the procedures will be thoroughly described in a forthcoming paper. Here we summarize the main points.

We use the raw "corrected frames" (`fpC`, bias and flat-field corrected) publicly available in the Third Data Release of the SDSS (DR3; Abazajian et al. 2005). Steps 1 and 2 rely on the centroid calculations and on the photometric calibrations provided by the DR3 catalogs and are performed using standard IRAF tasks. A bicubic spline interpolation is used to shift images. Regarding step 3, we note that an ideal mask should

[5] In one case the best possible match is within 0.3.

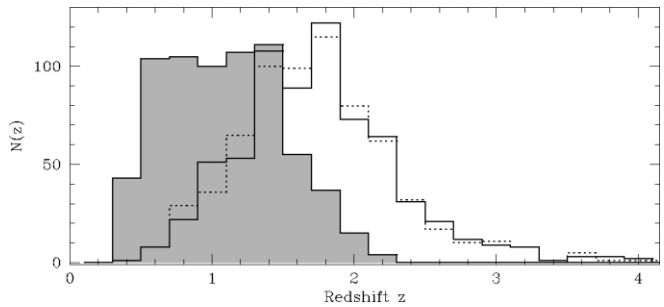

FIG. 1.—Redshift distribution of Mg II absorbers with $W_0 > 0.8$ Å (*shaded histogram*), of their background quasars (*solid histogram*), and of the reference quasars (*dotted histogram*).

retain only the QSO and the absorbing galaxy in each image, while blanking out completely all other sources in order to minimize the background noise. In practice, we design our masking algorithm to leave the QSO unmasked and to blank all sources that are likely to be in the foreground with respect to the absorber. For each QSO we create three independent masks in the *g*, *r*, and *i* bands, which are eventually combined in the final mask. In each band, a first mask is obtained from the segmentation image output by SExtractor (Bertin & Arnouts 1996) for a *clean* image of the field, from which we have subtracted the deblended "Atlas Image" of the QSO produced by the `photo` pipeline (Lupton et al. 2001). This step ensures optimal deblending of sources from the QSO and leaves the QSO unmasked. We retain the masks for all objects with a flux exceeding that expected from Bruzual & Charlot's population synthesis models (Bruzual & Charlot 2003, hereafter BC03) for an extreme case of a luminous blue galaxy: a stellar population with $M_i = -22.0$ produced by a burst 10^7 Gyr long, observed immediately after the burst end at the redshift of the absorber. Fainter objects are left unmasked. Our tests have shown that the final results do not critically depend on the assumed spectral energy distribution. Finally, the masks in the three bands are combined, and conservative masks are applied to all objects classified as stars by `photo` with $r < 20.0$.

After subtracting the background value evaluated on the masked image in an annulus between 200 and 250 pixels, the original images are shifted, intensity-calibrated, and averaged, excluding all masked pixels. Azimuthally averaged surface brightness (SB) profiles are extracted in a series of circular apertures, which are optimized to integrate on larger areas at larger radii. A more accurate background level for these profiles is recomputed on the stacked image between 100 and 150 pixels. The complete covariance matrix of the extracted background-subtracted SB profile is evaluated using the jackknife technique.

3.1. *Subtracting the Effective PSF*

To isolate the excess light due to intervening absorbers, the mean point-spread function (PSF) must be subtracted. The PSF depends on several parameters, such as the time of the observation, the position on a given camera column, and the color of the object. In order to build an effective PSF that is representative of the flux-averaged PSF of our QSOs extended to large angular distances, we stack stars selected to match each individual QSO. We first require stars to be observed in the same observing run and same camera column as the QSO. These stars are then ranked to minimize a combination of the following quantities: (1) the difference of Gaussian FWHM

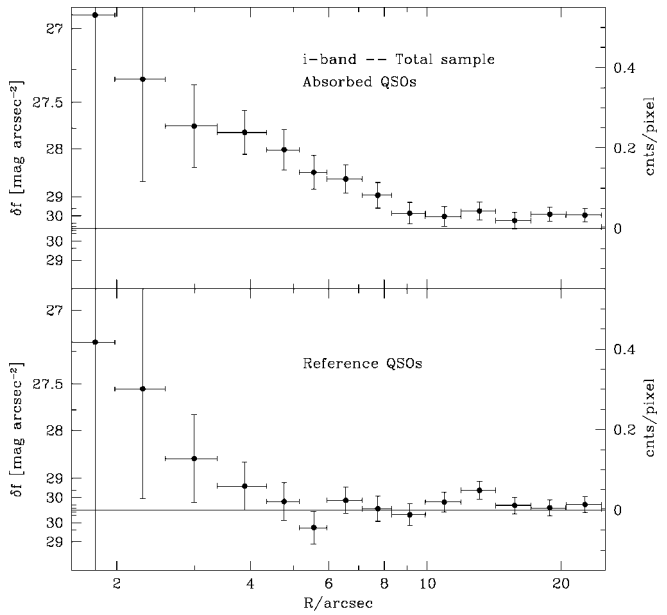

FIG. 2.—The *i*-band residuals (QSO minus PSF) as a function of radius *R* for the absorbed QSOs (*top*) and the reference unabsorbed QSOs (*bottom*). The *y*-axis scale is linear in flux intensity, as indicated on the right side (arbitrary count units per pixel). On the left the corresponding levels of the surface brightness excess or deficit are reported in mag arcsec^{-2}. The horizontal solid line indicates the background level. Error bars were computed with a jackknife algorithm.

with respect to the QSO, (2) the angular separation from the QSO, and (3) the differences in colors with respect to those of the QSO. To map the PSF with reasonable S/N at large distances, bright unsaturated stars are also preferred ($r < 17.0$ mag is always required). For each QSO in each band, the star that best fulfills all these criteria is chosen. To obtain the correct flux-weighted average PSF, the intensity of each star is rescaled to the same intensity of the corresponding QSO before stacking.

4. RESULTS

In Figure 2, we show the SB residuals measured in the *i* band after the PSF subtraction for the sample of 681 QSOs with absorbers (*top*) and for the reference QSO sample (*bottom*). The stacked PSFs are normalized with respect to the QSO profiles within an aperture of 4 pixels (1.″6). The vertical scale is linear in flux intensity, and the horizontal solid line is the background level. The left vertical axis displays the surface brightness in magnitudes per square arcsecond (in excess or deficit). Error bars are computed from the jackknife covariance matrix and include the budget from the background uncertainty. Central normalization uncertainties are found to be negligible. We note that within ~4″ both profiles display SB excesses: these systematic departures from the stellar PSF are due to reduced efficiency of source deblending close to the QSO and, partly, to the presence of the QSO host galaxy. However, we see very clearly that from 3″ outward the SB excess is significantly larger for absorbed QSOs. In particular, between 4″ and 8″ the absorbed QSOs display positive SB excesses that are significant at the 2–4 σ level each, while the profile of the reference QSOs is fully consistent with the background level. Similar results are found for the *r* and *g* bands as well. Note that galaxies that produce undetected absorbing systems at different redshifts are expected to be present with the same statistically uniform surface density as in the background. Therefore, the SB excess in the absorbed with respect to the reference QSOs are solely due to galaxies related to the selected absorption systems.[6]

In Table 1, we report the fluxes obtained by integrating the PSF-subtracted SB within 1.″6 and 10″ (~80 kpc in the z_{abs} interval considered) for the absorbed QSOs in the *g*, *r*, and *i* bands (cols. [2], [4], and [6], respectively, in magnitudes). The attached random errors (1 σ) are computed by propagating the errors on the residual SB profiles using the complete jackknife covariance matrix. In columns (3), (5), and (7), we report the systematic shifts that must be applied to the raw magnitudes integrated on the absorbers samples to correct for the bias in the inner 5″, as measured from the reference sample. Corresponding 1 σ upper and lower limits for this correction are also attached. Measurements are reported for the whole sample (681 QSOs) and for three subsamples of absorber systems binned in z_{abs}: $0.37 < z_{abs} \leq 0.82$, $0.82 < z_{abs} \leq 1.26$, and $1.26 < z_{abs} \leq 2.3$. Assuming the best estimated value for the systematic corrections, for the complete sample we have ~4 σ detection in *g* and *r* bands, and 6 σ in *i*. However, even with the most conservative corrections our detections are significant at 2.9 σ (*g* and *r*) and 5.3 σ (*i*). As expected, looking at the three redshift bins, we note that the signal is clearly dominated by the low-z_{abs} one. For this subsample the significance is 2.6 σ in *g*, 5.6 σ in *r*, and 9.4 σ in *i*. In the two higher redshift bins, the detections in individual bands are not statistically significant; however, the best estimates we derive are consistent with the dimming determined by the larger distance.

We now focus on the low-z_{abs} subsample to derive more physical information about the absorbing galaxies. In order to check whether the signal is dominated by a few anomalously bright objects, we have computed the luminosity function (LF) of all resolved sources below the masking threshold around the absorbed QSOs and statistically subtracted the analogous LF in the *reference* QSOs fields. We find that less than 5% of the flux is contributed by galaxies that are more than 2 mag brighter than the average values given in Table 1, while 80% is contributed by objects brighter than the average. The properties we derive are thus well representative of the *luminosity-*

[6] We cannot exclude, however, the possibility that more than one galaxy per absorber contributes to the signal. This might be the case if absorbing galaxies preferentially reside in groups.

TABLE 1
INTEGRATED MAGNITUDES OF QSO ABSORBERS

	g BAND		*r* BAND		*i* BAND	
SAMPLE (1)	$m(<10'')$ (2)	Δm Sys. (3)	$m(<10'')$ (4)	Δm Sys. (5)	$m(<10'')$ (6)	Δm Sys. (7)
All	$23.90^{-0.18}_{+0.22}$	$+0.13^{-0.13}_{+0.24}$	$22.98^{-0.14}_{+0.16}$	$+0.39^{-0.12}_{+0.15}$	$22.31^{-0.11}_{+0.12}$	$+0.28^{-0.08}_{+0.08}$
$z_{abs} \leq 0.82$	$23.76^{-0.28}_{+0.38}$	$+0.00^{-0.00}_{+0.12}$	$22.25^{-0.13}_{+0.16}$	$+0.10^{-0.10}_{+0.11}$	$21.40^{-0.08}_{+0.09}$	$+0.15^{-0.06}_{+0.05}$
$0.82 < z_{abs} \leq 1.26$	$24.55^{-0.48}_{+0.90}$	$+0.17^{-0.17}_{+0.68}$	$23.51^{-0.39}_{+0.59}$	$+1.03^{-0.48}_{+0.90}$	$23.63^{-0.47}_{+0.84}$	$+0.74^{-0.53}_{+1.10}$
$z_{abs} > 1.26$	$23.63^{-0.24}_{+0.30}$	$+0.45^{-0.33}_{+0.78}$	$23.69^{-0.32}_{+0.47}$	$+1.21^{-0.66}_{+1.96}$	$23.09^{-0.36}_{+0.52}$	$+0.72^{-0.35}_{+0.51}$

weighted average galaxy emission associated with absorbing systems.

From the photometric data presented above we derive colors within a 10″ aperture: $g-r = 1.41 \pm 0.35\ ^{+0.16}_{-0.11}$ and $r-i = 0.80 \pm 0.16\ ^{+0.13}_{-0.11}$ (the first uncertainty is random error on the direct measure; the second accounts for errors on the systematic correction). By neglecting the distribution of absorbers in redshift and assuming the median redshift of the sample, the comparison with BC03 models of solar-metallicity dust-free single stellar populations indicates that the luminosity-weighted average spectral energy distribution (SED) of Mg II–absorbing galaxies is dominated by fairly young stellar populations (~500 Myr old), with a rest-frame *r*-band absolute magnitude of about −21. The inferred rest-frame $B-K$ value is about 2.5 mag, which is compatible with although slightly bluer than the value found by Steidel et al. (1994) using direct imaging and spectroscopic follow-up. A more sophisticated analysis, in which we compare the observed colors with the *z*-folding of UV-optical galaxy templates (from Kinney et al. 1996) normalized to a fixed M_i, confirms that the "average" absorbing galaxy has a SED similar to local intermediate spirals (Sb–c). More details will be presented in a forthcoming paper.

5. CONCLUSIONS AND OUTLOOK

In this Letter, we have used a sample of 681 SDSS EDR QSOs with Mg II absorption lines ($W_0 > 0.8$ Å) to demonstrate the feasibility of studying the statistical photometric properties of galaxies associated with Mg II–absorbing clouds with the SDSS. By stacking images of quasars and subtracting the PSF, we have obtained significant detections (up to 9.4 σ in *i* band for the low-redshift subsample) of surface brightness excesses around QSOs with strong Mg II absorbers in the *g*, *r*, and *i* bands. Systematic biases are measured and removed with 10% to ~20% accuracy (for the total and low-z_{abs} samples) by using a control sample of QSOs without strong absorbers.

As expected, the measured excess light decreases as a function of absorber redshift. At $z \sim 0.6$, the mean colors ($g-r = 1.4$ and $r-i = 0.8$) indicate the presence of relatively young stellar populations and are consistent with the typical absorbing galaxy's resembling a local Sb–c spiral. The average luminosity per absorber within ~80 kpc impact parameter is similar to L_*. Both results are compatible with the previous finding by Steidel et al. (1994). A detailed analysis of impact-parameter distributions and constraints on the corresponding stellar populations will be presented in a forthcoming paper.

Previously, the largest photometric study of Mg II–absorbing galaxies was limited to ~60 low-redshift systems (Steidel et al. 1994), because of the expensive deep imaging and spectroscopic follow-up. Our technique allows the study of much larger samples: in this Letter we have analyzed a sample more than 10 times larger, and it will be soon applied to the SDSS absorber database (D. G. York et al. 2005, in preparation)—an order of magnitude larger. Although the statistical nature of our method makes it very difficult to study the real intrinsic variance of the absorbing galaxy properties, it can provide robust statistical results and also minimize the problem of confusion due to chance line-of-sight superposition of galaxies. Moreover, this technique can be applied to different absorption-line species (Fe I, Fe II, C IV, damped Lyα absorbers, etc.) to measure their impact parameters and investigate their spatial distribution in the gas around galaxies. Finally, it can also be used to investigate the properties of intrinsic absorber systems and quasar host galaxies.

We thank the anonymous referee for comments that have greatly improved the Letter, and Jim Gunn and Masataka Fukugita for useful discussions. B. M. acknowledges the support of the Florence Gould Foundation. Funding for the creation and distribution of the SDSS Archive has been provided by the Alfred P. Sloan Foundation, the Participating Institutions, the National Aeronautics and Space Administration, the National Science Foundation, the US Department of Energy, the Japanese Monbukagakusho, and the Max Planck Society.

REFERENCES

Abazajian, K., et al. 2005, AJ, 129, 1755
Bahcall, J. N., & Spitzer, L., Jr. 1969, ApJ, 156, L63
Bergeron, J., & Boissé, P. 1991, A&A, 243, 344
Bertin, E., & Arnouts, S. 1996, A&AS, 117, 393
Bruzual, G., & Charlot, S. 2003, MNRAS, 344, 1000 (BC03)
Churchill, C. W., Kacprzak, G. G., & Steidel, C. C. 2005, in IAU Colloq. 199, Probing Galaxies through Absorption Lines, ed. P. R. Williams, C. Shu, & B. Ménard (Cambridge: Cambridge Univ. Press), in press (astro-ph/0504392)
Churchill, C. W., Mellon, R. R., Charlton, J. C., Jannuzi, B. T., Kirhakos, S., Steidel, C. C., & Schneider, D. P. 2000, ApJS, 130, 91
Kinney, A. L., Calzetti, D., Bohlin, R. C., McQuade, K., Storchi-Bergmann, T., & Schmitt, H. R. 1996, ApJ, 467, 38
Lupton, R. H., Gunn, J. E., Ivezić, Ž., Knapp, G. R., Kent, S., & Yasuda, N. 2001, in ASP Conf. Ser. 238, Astronomical Data Analysis Software and Systems X, ed. F. R. Harnden, Jr., F. A. Primini, & H. E. Payne (San Francisco: ASP), 269
Nestor, D. B., Turnshek, D. A., & Rao, S. M. 2005, ApJ, 628, 637
Schneider, D. P., et al. 2002, AJ, 123, 567
Steidel, C. C., Dickinson, M., & Persson, S. E. 1994, ApJ, 437, L75
Stoughton, C., et al. 2002, AJ, 123, 485 (erratum 123, 3487)
York, D. G., et al. 2000, AJ, 120, 1579
Zibetti, S., White, S. D. M., & Brinkmann, J. 2004, MNRAS, 347, 556
Zibetti, S., White, S. D. M., Schneider, D. P., & Brinkmann, J. 2005, MNRAS, 358, 949